Evolution of itinerant electron magnetism in the (Sc, Nb)Fe_2 system in spin-fluctuation theory

S. El Bidaoui [1], L. V. B. Diop [2] and O. Isnard [1]
[1] *Université Grenoble Alpes, Institut Néel, CNRS, BP166X, 38042 Grenoble Cédex 9, France*
[2] *Université de Lorraine, CNRS, IJL, F-54000 Nancy, France*

(Received 13 July 2024; revised 27 September 2024; accepted 14 November 2024; published 2 December 2024)

The magnetic behavior of the (Sc, Nb)Fe_2 series of intermetallic compounds was thoroughly investigated in the ordered ferromagnetic state as well as in the paramagnetic regime. The magnetic moment of the Fe sublattice was determined from 4 K up to the magnetic ordering temperature while the analysis of the paramagnetic state yielded the determination of the effective paramagnetic moment and Curie-Weiss temperature. The number of carriers was estimated below and above the Curie point so as to discuss the degree of itinerancy of Fe magnetism in the (Sc, Nb)Fe_2 system. The experimental results were analyzed in the frame of Kuz'min's model describing the temperature dependence of the spontaneous magnetization, and Takahashi's theory of spin fluctuations. It is shown that both Curie temperature and paramagnetic Curie-Weiss temperature decrease linearly upon increasing Nb content. The longitudinal spin fluctuations progressively increase for the richest Nb compositions, by contrast, transverse spin fluctuations dominate for the parent compound $ScFe_2$. Furthermore, a reduction in ferromagnetic interactions upon Nb for Sc substitution is observed, resulting in an evolution from a short-range ferromagnet for $ScFe_2$ to systems with competing exchange interactions for Nb-rich composition. Nb-rich (Sc, Nb)Fe_2 compounds evolve progressively toward the weakly ferromagnetic limit. Spin-fluctuation parameters have been determined from magnetic measurements using Takahashi's model. We report an evolution from mostly localized magnetic character of Fe moments to a strongly delocalized one upon increasing the Nb content along the $Sc_{1-x}Nb_xFe_2$ series of compounds. In the composition range $0 \leqslant x \leqslant 0.22$ the degree of itinerancy is nearly constant, whereas for $x > 0.22$ it is remarkably dependent upon the Nb concentration.

DOI: 10.1103/PhysRevB.110.224406

I. INTRODUCTION

Fe-based Laves phases have been known for decades and have been the matter of extensive studies [1]. They have attracted abundant interest from the modern technological applications viewpoint as well as from the fundamental research side, offering a plethora of tunable structural, electronic, and magnetic properties. Laves-type intermetallic materials are successfully utilized in a surprisingly broad range in functional applications comprising hydrogen storage alloys, for wear- and corrosion-resistant coatings in corrosive atmospheres and at high temperatures, for creep strengthening of high-temperature steels, and as magnetomechanical sensors and actuators, to name but a few [2]. In addition, colossal negative thermal expansion induced by magnetic phase competition, and large magnetocaloric effect as well as a giant hydrogen/deuterium isotope effect have recently been reported for some Laves phase intermetallics [3–6]. The mere fact that Laves-type intermetallic compounds have such a large variety of different functional properties makes this material family outstanding.

Laves family of compounds AFe_2, where A can be a $3d$, $4d$, $5d$, or rare-earth element, exhibit various types of crystal structure and magnetic order depending upon the species at the A site. Binary Laves phase alloys are made of three parent members: the C14 hexagonal $MgZn_2$ type ($P6_3/mmc$), the C15 cubic $MgCu_2$ type (Fd-$3m$), and the C36 hexagonal $MgNi_2$ type ($P6_3/mmc$) crystallographic structures. We will focus our attention on Laves-type intermetallic compounds crystalizing in the C14 $MgZn_2$-type atomic arrangement. In the hexagonal C14 crystal structure, A atoms occupy one single crystallographic site $4f$ with an axial symmetry $3m$, generated by (1/3, 2/3, z). The Fe atoms are located on two inequivalent Wyckoff positions: $2a$ (0, 0, 0) with an axial symmetry $\bar{3}m$ and $6h$ with the point symmetry $mm2$, generated by (x, $2x$, 1/4). The crystal lattice has a layered structure as shown in Fig. 1. One layer is formed by A atoms at $4f$ position and $2a$ Fe sites. Another layer consists of hexagonal sheet of Fe at $6h$ site and characterized by two kagome networks ($\perp$ to the high-symmetry axis c). In terms of crystallography, the A atoms reside in Fe cages and there are two distinct types of Fe atomic positions which behave differently from a magnetic point of view (Fig. 1).

In the hexagonal C14 Laves structure, for instance, $TiFe_2$ and $TaFe_2$ are antiferromagnets [7–9], while $HfFe_2$ and $ScFe_2$ [10,11] present a ferromagnetic ground state. Interestingly, $NbFe_2$ is a rare itinerant system close to magnetic quantum criticality [12–18]. It is well established that as a function of the nonthermal control parameter such as chemical doping in $Nb_{1-y}Fe_{2+y}$, that is as function of the Nb/Fe stoichiometry, three different ground-state phases are traversed across a narrow compositional range [14,15]. Slightly off-stoichiometric compounds (both towards the Fe-rich and the Nb-rich side) are weak ferromagnets in the low-temperature region. At or very close to stoichiometry, spin-density wave (SDW), or an antiferromagnetic (AFM) order develops on top of the ferromagnetic (FM) phase. Additionally, in between stoichiometric

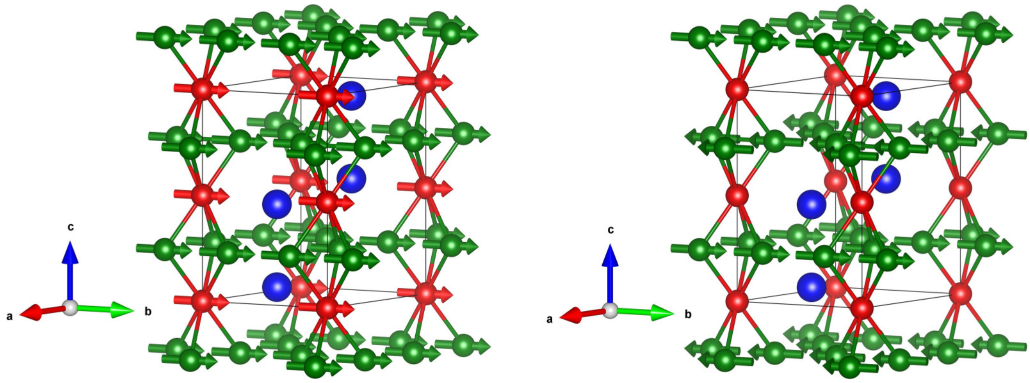

FIG. 1. Schematic representation of the crystal and magnetic structures of AFe_2 compounds with a hexagonal $MgZn_2$-type atomic arrangement [e.g., (Hf, Ta)Fe_2 family]. Left (right) figure corresponds to the ferromagnetic (antiferromagnetic) ordering. The A atoms at $4f$ site are represented by blue balls. The $2a$ and $6h$ Fe atoms are depicted in red and green, respectively. The arrows indicate the magnetic moments.

concentration and the Nb-rich side, a quantum critical point–regime emerges where the SDW state vanishes and non-Fermi-liquid behavior is observed [12,13,16].

A first-order magnetic transition between two ferromagnetic states with different degrees of localization has been evidenced in the (Sc, Ti)Fe_2 system [19–21]. (Hf, Ta)Fe_2 and (Hf, Nb)Fe_2 intermetallics exhibit multiple temperature-induced phase transitions from ferromagnetic (FM) to antiferromagnetic (AFM) order and then to the paramagnetic (PM) state upon heating [9,22]. A common feature to all the aforementioned compounds is that in the FM state the magnetism originates from the two Fe sublattices, $2a$ and $6h$ sites, both carrying a sizable magnetic moment (Fig. 1). By contrast, the AFM ordering is only due to 3/4 of the Fe atoms, namely those occupying $6h$ Wyckoff positions, while Fe atoms located on $2a$ crystal sites are not magnetically ordered [7,23,24]. In the rather complex AFM magnetic structure $6h$ spins are ferromagnetically aligned within the same layer but with opposite orientations between successive layers (Fig. 1). Since the $2a$ crystallographic site forms an inversion center for the $6h$ sublattice, the molecular field experienced by the $2a$ site from $6h$ spins vanishes by symmetry. Therefore, $2a$ Fe atoms show null ordered magnetic moments or null hyperfine fields in neutron diffraction and Mössbauer spectroscopy studies, respectively [7,23,24]. Pressure-induced collapse of ferromagnetism has been observed for (Hf, Ta)Fe_2 [9]. A detailed investigation of the interatomic Fe-Fe exchange coupling constants and their dependence as a function of unit-cell parameters unveiled that the FM interaction with the first shell is significantly decreased upon shrinkage of the a-cell dimension [25]. Another noteworthy finding of the theoretical calculations in Ref. [25] is that the Fe$6h$ − Fe$6h$ exchange coupling is always positive, i.e., these interactions will favor a FM spin arrangement within the atomic plane containing the Fe$6h$ positions with Fe$6h$ as near neighbors. Most recently, nonconventional thermal effects across the FM-AFM first-order magnetic phase transition were observed in the Ta-doped $HfFe_2$ intermetallic [26]. Such peculiar thermal effects result in warming (cooling) when heat is extracted from (supplied to) the magnetic material, hence providing indisputable evidence of metastable supercooled AFM- and superheated FM states [25,26]. The magnetic phase diagram of the (Hf, Ta)Fe_2 system [9,27,28] has been qualitatively explained on the basis of the Moriya-Usami theoretical model of spin fluctuations in itinerant electron systems in which the antiferromagnetic and ferromagnetic components of spin-fluctuation modes coexist [29].

The discovery of these intriguing physical phenomena has stimulated the scientific community and triggered intense research worldwide. It is noteworthy that in the above-mentioned examples unexpected magnetic features emanate from the Fe sublattice. This clearly demonstrates the complex magnetic behavior of Fe sublattice in Laves phases, a magnetism due to the $3d$ itinerant electrons.

Materials exhibiting itinerant electron magnetism have attracted considerable interest over the years [30–32]. The theoretical works on itinerant electron ferromagnetic materials can be traced back to studies by Bloch [33], Slater [34,35], and Stoner [36,37] starting in the late 1920s. Stoner's theory of itinerant electron ferromagnetism was based on the Hartree-Fock and mean-field approximations. In the $3d$ metals and their intermetallic compounds, these early theories describe the magnetic properties of the ground state of itinerant electron ferromagnets such as not integer values of the observed spontaneous moment. However, they encounter difficulties in explaining finite-temperature magnetic behavior such as Curie-Weiss law of the magnetic susceptibility above the ferromagnetic ordering temperature. Rhodes and Wohlfarth [38] proposed a plot based on experimental data to distinguish between systems obeying localized magnetism and those displaying itinerant magnetism. Later, Moriya developed the theory of self-consistent renormalization (SCR) [39,40], which successfully explained many magnetic phenomena in materials with itinerant electron magnetism. Moriya considered the correlation effect overlooked in Stoner's theory, in addition to accounting for the effect of temperature on spin fluctuations. A complementary theory to Moriya's one was subsequently introduced by Takahashi [31,32,41]. Takahashi's approach is based first on the conservation of the sum of zero and thermal spin fluctuations as a function of temperature, and second on the temperature dependence of the magnetic free-energy coefficients. This theoretical model shows good agreement with experimental results, thereby supporting its efficiency in describing the magnetic properties at low temperature and around magnetic transitions that could not be explained by Moriya's theory. Indeed, Takahashi established a relationship based on the spin-fluctuations theory, giving a theoretical background to the evolution of the degree of itinerancy of itinerant electron magnetism originally pointed out by Rhodes and Wohlfarth. Initially applied to weakly ferromagnetic systems such as MnSi, $ZrZn_2$, $Y(Co, Al)_2$, and $Sc(Co, Al)_2$ [32,41,42], recent experimental studies have demonstrated the applicability of Takahashi's theory to describe the magnetic behavior of itinerant electron in various ferromagnetic systems [30,43,44].

With this growing interest, we aim to apply Takahashi's spin-fluctuation theory on $(Sc, Nb)Fe_2$ model system in order to get a deeper insight into their magnetic properties and also to assess the validity of this theory for such magnetic system. The pseudobinary compounds $(Sc, Nb)Fe_2$ constitute a phenomenal playground for materials physics due to the strong coupling between lattice and spin degrees of freedom in these systems and the extreme sensitivity of their physical properties to relatively weak external stimuli or to chemical pressure [45]. In the present study, the internal pressure is used as a driving force to tune and control the magnetic properties of the $(Sc, Nb)Fe_2$ series of compounds. Laves phases $(Sc, Nb)Fe_2$ have been purposefully chosen since the nonthermal control parameter such as element substitution induces isomorphic lattice evolution (without change of crystal symmetry) and their low-temperature magnetic ground state has been most recently investigated in detail [45]. This $(Sc, Nb)Fe_2$ system also attracted our interest since it offers the unique evolution from pure ferromagnetic ground state towards magnetic quantum criticality. In this paper, we report a systematic study of the magnetic properties in the magnetically ordered state as well as in the paramagnetic state. The results will be discussed in light of the Rhodes-Wohlfarth plots [38,46] and using Takahashi's theory of itinerant electron magnetism [31,32,41] in order to analyze the behavior of $Sc_{1-x}Nb_xFe_2$ compounds and quantify the evolution of the Fe-*3d* electron magnetism along the series.

II. EXPERIMENTAL TECHNIQUES

$Sc_{1-x}Nb_xFe_2$ ($0 \leqslant x \leqslant 1$) intermetallic compounds were prepared by electric arc melting of high-purity chemical elements. Stoichiometric components were melted in pure argon atmosphere to prevent oxidation. The so-obtained ingots were subsequently annealed in a resistive furnace at 1000 °C for 1 week and then quenched in water. For such heat treatment, the samples were placed in zirconia crucibles and inserted into quartz tubes sealed under 0.2-bar argon.

The phase identification and characterization (crystal structure and chemical composition) of $(Sc, Nb)Fe_2$ intermetallic compounds were performed using x-ray powder diffraction and scanning electron microscopy associated with energy dispersive x-ray spectroscopy. Rietveld refinements of the x-ray-diffraction patterns at room temperature showed that the $(Sc, Nb)Fe_2$ series of alloys was single phase and crystallized in the hexagonal $MgZn_2$-type structure, also referred to as C14 ($P6_3/mmc$ space group). Further details on the synthesis, crystal structure, and magnetic properties in the ordered state of $(Sc, Nb)Fe_2$ intermetallics can be found in Ref. [45].

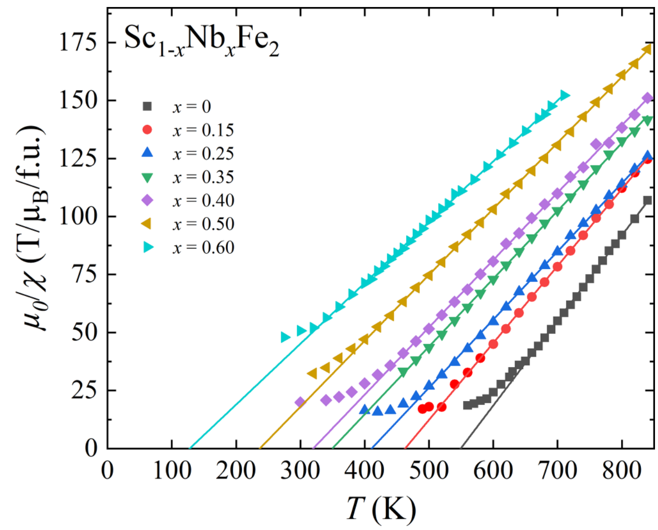

FIG. 2. Thermal evolution of the inverse susceptibility for $Sc_{1-x}Nb_xFe_2$ compounds.

Magnetization measurements were carried out on pieces (weight ranging between 0.1 and 0.3 g) using the extraction magnetometers installed at the Institute Néel (operating at high: 200–850 K and low: 1.8–300 K temperatures and magnetic field of up to 7 and 10 T, respectively). The magnetometers are described in detail in Ref. [47].

III. RESULTS AND DISCUSSION

A. Paramagnetic state

The low-temperature magnetic properties of the $(Sc, Nb)Fe_2$ series of intermetallic compounds, in the ferromagnetic state, were presented in our previous paper [45]. The Curie temperature T_C and spontaneous magnetization M_S values are summarized in Table I. T_C decreases continuously from 524 K for $x = 0.1$ to 120 K for $x = 0.6$, whereas the composition dependence of M_S is nonmonotonic, i.e., M_S slightly increases in the concentration range $0 \leqslant x \leqslant 0.22$, followed by a sharp decrease down to the extreme composition $NbFe_2$, where no magnetic order was observed.

In order to investigate the magnetic behavior of Fe in the paramagnetic regime, the magnetic susceptibility was determined from the magnetization isotherms recorded at temperatures above the Curie point. Figure 2 illustrates the thermal evolution of the inverse susceptibility of $Sc_{1-x}Nb_xFe_2$ alloys. The reciprocal magnetic susceptibility for compounds with $0 \leqslant x \leqslant 0.6$ obeys Curie-Weiss law. The effective paramagnetic moment p_{eff} was deduced from the Curie constant C. The corresponding values of C, p_{eff}, and the paramagnetic Curie temperature θ_{CW} are given in Table I. The positive values of θ_{CW} indicate a predominance of ferromagnetic interactions in this composition range. As it can be clearly seen from Fig. 3, the θ_{CW} values are slightly larger than the T_C values. The highest θ_{CW} value of 550 K is obtained for $ScFe_2$. θ_{CW} decreases progressively down to 128 K for $x = 0.6$, indicating a strong reduction of the mean magnetic exchange energy upon Nb for Sc substitution. The results reveal that the effective magnetic moment is much less sensitive to the substitution. A slight increase is observed from 2.47 μ_B/Fe

TABLE I. Magnetic properties of $Sc_{1-x}Nb_xFe_2$ intermetallics. M_S is the spontaneous magnetization at 4 K; T_C is Curie temperature; θ_{CW} is paramagnetic Curie temperature; C is Curie constant; p_{eff} is effective moment; p_c/p_s is Rhodes-Wohlfarth ratio; B_{ex} exchange field, and s is the shape parameter.

x	M_S (μ_B/f.u.)	T_C (K)	θ_{CW} (K)	C (μ_B K/f.u. T)	p_{eff} (μ_B/Fe)	p_c/p_s	B_{ex} (T)	s
0	2.32 (5)	530 (5)	550 (5)	2.73	2.47	1.45	450	0.77(5)
0.10	2.44 (5)	524 (5)	524 (5)	2.96	2.57	1.44	432	0.80(4)
0.15	2.47 (5)	443 (5)	466 (5)	3.02	2.60	1.44	362	1.23(4)
0.17	2.45 (5)	438 (5)	466 (5)	3.06	2.61	1.47	351	1.20(12)
0.175	2.57 (5)	432 (5)	460 (5)	3.15	2.65	1.43	352	1.54(7)
0.18	2.59 (5)	434 (5)	465 (5)	3.23	2.69	1.44	348	1.29(7)
0.20	2.59 (5)	420 (5)	450 (5)	3.04	2.61	1.38	358	1.60(4)
0.22	2.66 (5)	417 (5)	450 (5)	3.43	2.77	1.46	323	1.58(3)
0.25	2.51 (5)	383 (5)	410 (5)	3.41	2.76	1.55	282	1.76(3)
0.30	2.38 (5)	345 (5)	390 (5)	3.27	2.70	1.58	251	2.04(5)
0.35	1.72 (5)	314 (5)	347 (5)	3.44	2.77	2.26	–	2.2(1)
0.40	1.17 (5)	240 (5)	315 (5)	3.49	2.79	3.36	–	2.48(10)
0.50	0.43 (5)	170 (5)	225 (5)	3.59	2.83	9.32	–	–
0.60	0.16 (5)	120 (5)	128 (5)	3.86	2.94	26.27	–	–

for $x = 0$ to 2.94 μ_B/Fe for Nb-rich compound ($x = 0.6$). The obtained values are much smaller than those found in other Fe-rich binary systems such as Y_2Fe_{17} (3.97 μ_B/Fe) [48], Th_2Fe_{17} (4.40 μ_B/Fe), and Fe_3C (3.89 μ_B/Fe) [49], but they compare well with those reported for $Sc_{1-x}Ti_xFe_2$ ($x = 0.7$, 0.9, and 1) alloys $2.4 \leqslant p_{eff} \leqslant 3$ μ_B/Fe [50], and the value $p_{eff} = 2.99$ μ_B/Fe obtained for $HfFe_2$ compound [9].

The magnetic properties of the pseudobinary system $(Sc, Nb)Fe_2$ were analyzed on the basis of the Rhodes-Wohlfarth plot [38,46] which gives the p_c/p_s ratio of magnetic moments as a function of Curie temperature. Here, p_s is the number of magnetic carriers per atom in the ferromagnetic state deduced from the spontaneous magnetization, and p_c is the number of carriers in the paramagnetic state determined from the effective paramagnetic moment using the following relation: $p_{eff} = \mu_B\sqrt{p_c(p_c+2)}$.

It is established that Rhodes-Wohlfarth plot allows to distinguish between itinerant and localized magnetism [49,51]. In a material with localized moments, the ratio p_c/p_s amounts to 1. By contrast, in the case of itinerant moments $p_c/p_s > 1$. Figure 4 presents the evolution of the Rhodes-Wohlfarth ratio p_c/p_s vs T_C for $Sc_{1-x}Nb_xFe_2$ compounds. The p_c/p_s ratio for $ScFe_2$ equals 1.45 close to unity, indicating that this compound is close to the localized nature of the magnetic moments yet more delocalized than in elemental Fe. This ratio increases as a function of Nb concentration along the $Sc_{1-x}Nb_xFe_2$ series of intermetallics, denoting that the degree of itinerancy of Fe *3d* electron magnetism increases upon Nb for Sc substitution. Two regimes can be identified: below $x = 0.22$, the Rhodes-Wohlfarth ratio p_c/p_s remains nearly constant whereas above $x = 0.22$ it considerably increases, reaching a value of 26 for the compound with $x = 0.6$. According to the interpretation of the Rhodes-Wohlfarth curve, one can deduce that the evolution of the p_c/p_s ratio reflects a trend towards more and more delocalized magnetism upon Nb for Sc substitution

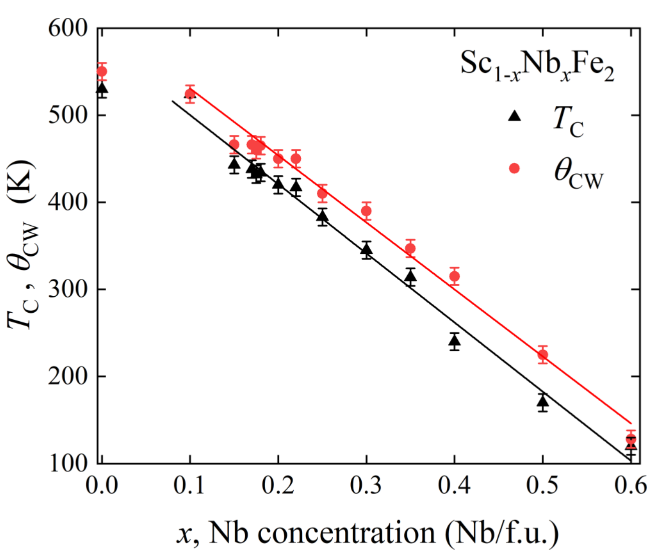

FIG. 3. Evolution of T_C and θ_{CW} as a function of Nb concentration for $Sc_{1-x}Nb_xFe_2$ compounds.

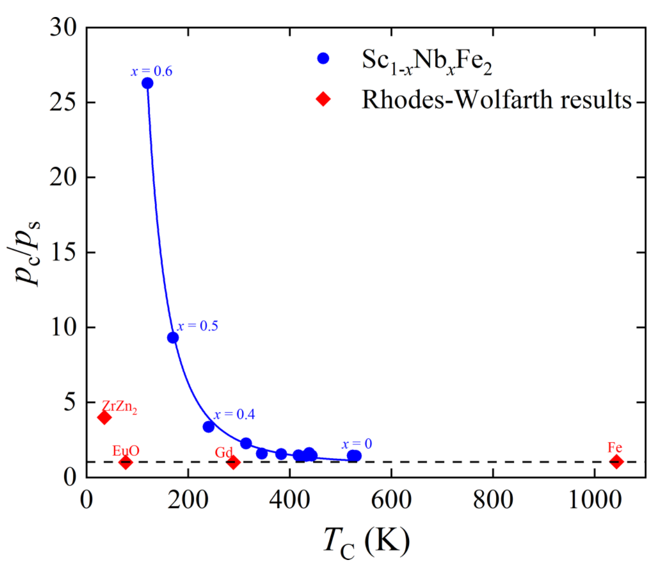

FIG. 4. Rhodes-Wohlfarth plot for $(Sc, Nb)Fe_2$ compounds. Dashed line corresponds to $p_c/p_s = 1$.

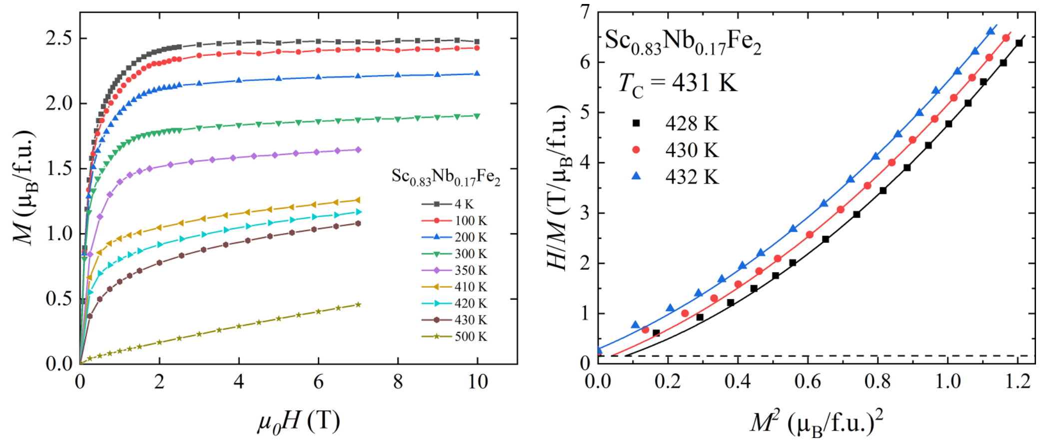

FIG. 5. Isothermal magnetization curves recorded at the indicated temperature (left) and corresponding Arrott-Belov plots for $Sc_{0.83}Nb_{0.17}Fe_2$ around the Curie temperature (right).

along the $Sc_{1-x}Nb_xFe_2$ series of intermetallic compounds. With the richest Nb composition being progressively closer to the weakly ferromagnetic limit, that is when the longitudinal spin fluctuations play an important role, contrary to the nearly localized case of $ScFe_2$ where the transverse spin fluctuations are expected to be dominant according to the self-consistent renormalized theory of Moriya [52]. Nishihara et *al.* [21] have reported a p_c/p_s ratio of 1.4 for $ScFe_{1.95}$, a value in very good agreement with our results. They have also shown that this ratio increases with Ti content in $Sc_{1-x}Ti_xFe_{1.95}$ intermetallics. Similar behavior has been observed in other Fe-based intermetallics, such as $Hf_{1-x}Ta_xFe_2$ [9] and $Th_2Fe_{17}C_x$ [49]. This indicates the effect of substitution or insertion of nonmagnetic element on the *3d* electron itinerant magnetism of Fe.

The exchange field is related to the Curie temperature and spontaneous magnetization by the following relationship:

$$B_{\text{ex}} = \frac{M_S\, T_C}{C}. \tag{1}$$

The values of B_{ex} derived from Eq. (1) for (Sc, Nb)Fe_2 intermetallics are listed in Table I. One can observe a tremendous diminution of the magnitude of the exchange field B_{ex}; a value of $B_{\text{ex}} = 450$ T is deduced for the parent compound $ScFe_2$ as compared to the value $B_{\text{ex}} = 251$ T for $x = 0.3$. For comparison purposes it is worth noting that the value of B_{ex} observed here for $ScFe_2$ ferromagnet is of the same order of magnitude as that reported for $HfFe_2$ ($B_{\text{ex}} = 466$ T) [53] but is at least twice smaller than the exchange field of Fe metal (1023 T).

B. Determination and temperature dependence of the spontaneous magnetization

At low temperatures the spontaneous magnetization M_S was determine from the magnetization isotherms by extrapolation to demagnetizing field, i.e., the crossing point of the linearly extrapolated low- and high-field portions of the isothermal magnetization curves. However, this simple technique becomes ambiguous near the Curie point and is no longer applicable since the magnetization curve becomes basically nonlinear. This difficulty is overcome by using, in the vicinity of the magnetic ordering temperature, a standard method developed independently by Belov and Georgia, and Arrott [54,55] and based on Landau's theory of second-order phase transitions. The Arrott-Belov procedure consists of plotting the isothermal magnetization curves as H/M vs M^2, as illustrated for $Sc_{0.83}Nb_{0.17}Fe_2$ in Fig. 5 (right panel). The data points of the upper portions of the Arrott-Belov graphs, situated well above the demagnetization line, were fitted with a degree-2 polynomial, and the intersections of the fits with the demagnetization line were taken as values of ${M_S}^2$. The T_C values obtained from the Arrott-Belov plots are in good agreement with those deduced from the thermomagnetic measurements (listed in Table I).

The spontaneous magnetization of (Sc, Nb)Fe_2 intermetallic compounds is plotted against temperature in Fig. 6. The solid lines are fits to the Kuz'min equation [56]:

$$\frac{M_S}{M_0} = \left[1 - s\left(\frac{T}{T_C}\right)^{3/2} - (1-s)\left(\frac{T}{T_C}\right)^{5/2}\right]^{\beta}. \tag{2}$$

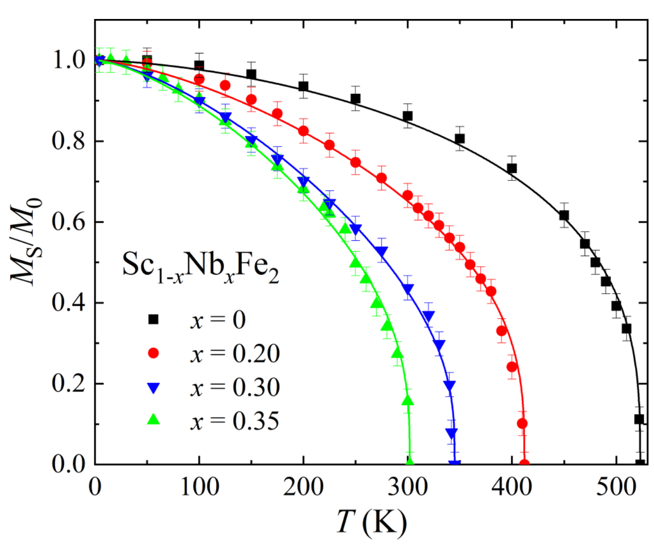

FIG. 6. Reduced spontaneous magnetization of $Sc_{1-x}Nb_xFe_2$ vs temperature. Dots correspond to data measured and the solid line is a fit to Kuz'min's Eq. (2).

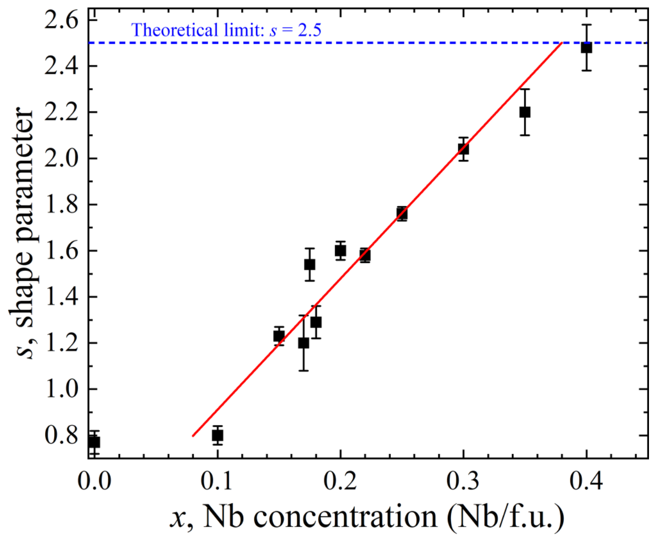

FIG. 7. Evolution of the shape parameter s as a function of Nb concentration along the $Sc_{1-x}Nb_xFe_2$ series.

Here, M_0 is the spontaneous magnetization at $T = 0$ K, T_C is the Curie temperature, β is a critical exponent, and s is a dimensionless parameter that characterizes the shape of the M_S (T) curve, referred to as the shape parameter ($0 < s < 5/2$) [56,57]. The critical exponent was fixed to a value of $\beta = 0.33$, and the obtained values for the shape parameter s are reported in Fig. 7. The s value varies from 0.77 to 2.48 for $x = 0$ and $x = 0.4$, respectively. According to Kuz'min [57], the shape parameter s is related to the intensity of exchange interactions. A s value greater than 0.8 denotes the presence of competing exchange interactions with low T_C. On the contrary, an s value less than 0.4 indicates ferromagnetic exchange interactions with very high T_C. An intermediate value $s = 2/3$ demonstrates the dominance of short-range interactions. In the (Sc, Nb)Fe_2 series of compounds, the observed behavior reflects the evolution from a short-range ferromagnetic system for $x = 0$ and $x = 0.1$ towards systems with competing exchange interactions as the Nb concentration increases. For $ScFe_2$, $s = 0.77$ is a typical value for iron (cobalt)-rich ferromagnets; for example: $s = 0.7$ for $Y_2Fe_{14}B$, YCo_5 [58] and $YCo_{11}FeB_6$ [59], $s = 0.8$ for $Y_2Fe_{14}Si_3$ [58]. It is noteworthy that the theoretical limit for the shape parameter s is 5/2. Above this upper bound of 5/2 the magnetic system is not a ferromagnet and Kuz'min's model is no longer valid. Detailed explanations for the shape of the temperature dependence of the spontaneous magnetization of a ferromagnet and factors determining this shape can be found in Refs. [56–58].

C. Analysis in the frame of Takahashi's theory of spin fluctuations

Takahashi [31,32,41,60] has developed a theory of spin fluctuations to overcome the difficulties encountered previously in Moriya's SCR theory. Takahashi's theory is based on the following assumptions [31,32]:

(1) Total spin-fluctuation amplitude conservation (TAC): this means that the average amplitude of the local spin squared on each magnetic site remains constant independent of temperature. It is also unaffected by external magnetic field. Moreover, the spin-fluctuation amplitude is the sum of the zero point and the thermal amplitudes.

(2) Global consistency in effect of magnetic field (GC): no assumptions are made for the magnetic isotherms in this theory, in contrast to the SCR theory, where the fourth-order coefficient of the free energy was assumed to be independent of temperature. The GC means that the magnetic isotherm is globally consistent with the first condition.

Depending on the studied case (ferromagnetic or local moment limit) and the magnetic state (ordered or paramagnetic state), Takahashi calculated the spin-fluctuation amplitude to describe magnetic isotherms. The validity of this theory for describing the magnetic properties of ferromagnetic compounds has been demonstrated by several experimental works [32,42,43,61,62]. In this section, (Sc, Nb)Fe_2 intermetallics are analyzed in the framework of Takahashi's theory in order to examine the composition dependence of the magnetic behavior.

According to this theoretical model, the variation of M^2 as a function of H/M is equivalent to the expansion of the free energy in the power of M up to the fourth-order term [60]. The magnetic free energy $F(M,T)$ can be written as follows [60]:

$$F\,(M,T) = F(0,T) + \frac{1}{2\,(g\,\mu_B)^2\,\chi}\,M^2 + \frac{\bar{F}_1}{4\,N_0^3\,(g\,\mu_B)^4}\,M^4 + \cdots, \tag{3}$$

where g is the gyromagnetic factor ($g = 2$), μ_B is the Bohr magneton, χ is the magnetic susceptibility of the material, N_0 is the number of magnetic atoms per mole [for (Sc, Nb)Fe_2, $N_0 = 2\,N_A$, where N_A is the Avogadro number], and $\bar{F}_1$ is the fourth expansion coefficient of the magnetic free energy in joules.

In the ground state, the magnetic-field dependence of the magnetization is obtained by deriving the free energy with respect to the magnetization $\frac{dF(M,T)}{dM} = H$:

$$\frac{H}{M} = \frac{1}{(g\,\mu_B)^2\,\chi} + \frac{\bar{F}_1}{N_0^3\,(g\,\mu_B)^4}\,M^2, \tag{4}$$

$$M^2 = \frac{N_0^3\,(g\,\mu_B)^4}{\bar{F}_1}\left(\frac{H}{M} - \frac{1}{(g\,\mu_B)^2\,\chi}\right). \tag{5}$$

Equation (5) is valid for high magnetic fields where the M^2 vs H/M curve is linear. The value of $\bar{F}_1$ can be estimated from the slope ζ of the Arrott-Belov plot of M^2 vs H/M at low temperatures. Figure 8 shows a low-temperature Arrott-Belov plot for $Sc_{0.83}Nb_{0.17}Fe_2$. The fourth-order expansion coefficient is deduced from the slope in the high-field region. F_1 values determined for the $Sc_{1-x}Nb_xFe_2$ series of compounds are listed in Table II. According to Takahashi's theory [32,41,60], the F_1 coefficient is approximately related to the two fluctuation parameters T_0 and T_A using Eq. (6). T_0 and T_A characterize the spectral width of the spin-fluctuation amplitudes in the energy space (or frequency space ω) and wave-vector space (or wave-number space q), respectively [32,41,60]. T_0 and T_A parameters can be directly estimated from inelastic neutron-scattering experiments or from nuclear magnetic resonance

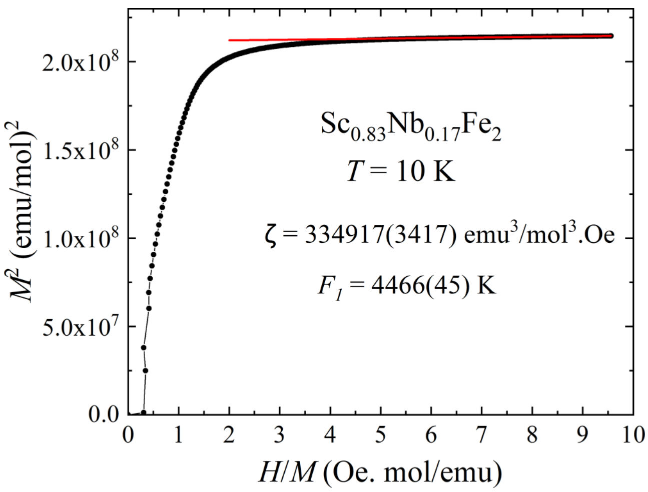

FIG. 8. Arrott-Belov plot M^2 vs H/M at 10 K for $Sc_{0.83}Nb_{0.17}Fe_2$. The red line corresponds to a fit according to Eq. (5).

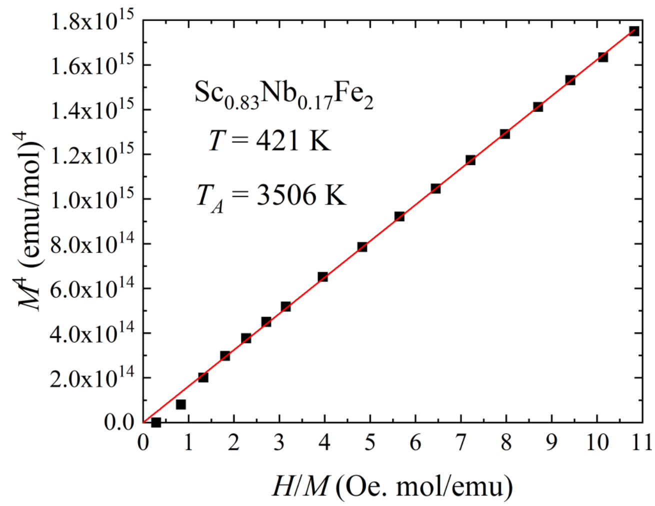

FIG. 9. M^4 vs H/M plot for $Sc_{0.83}Nb_{0.17}Fe_2$ in the critical region (at T = 421 K). The solid line corresponds to a fit according to Eq. (10).

(NMR) measurements [32,42,60,62]:

$$F_1 = \frac{2\,T_A^2}{15\,c\,T_0} = \frac{N_0^3\,(g\,\mu_B)^4}{k_B\,\zeta}. \qquad (6)$$

Here, $\bar{F}_1 = F_1 \times k_B$, $c = 1/2$ and k_B is Boltzmann's constant. The right-hand term in Eq. (6) is deduced from Eq. (5). Note that the coefficients F_1, T_0, and T_A are all expressed in kelvin. Let p_s be the magnetic moment per magnetic atom at $T = 0$ K in units of μ_B, defined by $p_s = M_S/N_0\ \mu_B$, where M_S is the spontaneous magnetization. Takahashi has demonstrated that due to the absence of thermal spin fluctuation in the ground state, the spontaneous magnetization can be written as follows:

$$p_s^2 \approx \frac{20\,T_0}{T_A}\,C_{4/3}\left(\frac{T_C}{T_0}\right)^{4/3}\left(\text{for } \frac{T_C}{T_0} \ll 1\right). \qquad (7)$$

Using Eqs. (6) and (7), we can obtain two relationships that allow us to define the parameters T_A and T_0 separately, as a function of the quantities known from the magnetic measurements F_1, p_s, and T_C:

$$\left(\frac{T_C}{T_0}\right)^{5/6} = \frac{p_s^2}{20\,C_{4/3}}\left(\frac{15\,c\,F_1}{2\,T_C}\right)^{1/2}, \qquad (8)$$

$$\left(\frac{T_C}{T_A}\right)^{5/3} = \frac{p_s^2}{20\,C_{4/3}}\left(\frac{2\,T_C}{15\,c\,F_1}\right)^{1/3}, \qquad (9)$$

where $C_{4/3} = 1.006\,089$.

Based on the GC assumption in the critical region, Takahashi has included the M^6 term (neglected in the SCR theory) in the Landau series expansion of the magnetic free energy [30,32]. This leads to the continuity of the magnetization at the Curie temperature. Consequently, the critical magnetic isotherm can be described by the following equation [32]:

$$\left(\frac{M}{M_0}\right)^4 = 3188\ \times (N_0\mu_B) \times \frac{\mu_B}{K_B} \times \frac{T_C^2}{T_A^3\,p_s^4}\left(\frac{H}{M}\right). \qquad (10)$$

Equation (10) indicates that magnetic isotherms in the critical region are linear. Using Eq. (10), we can estimate the value of T_A from the slope of the M^4 curves as a function of H/M around the critical temperature. The corresponding values are summarized in Table II under T_A^*. We exemplify in Fig. 9 the magnetic isotherm for $Sc_{0.83}Nb_{0.17}Fe_2$ at a temperature close to T_C. As it can be clearly seen from Fig. 9, the fitted curve is in excellent agreement with the experimental data. For $Sc_{0.83}Nb_{0.17}Fe_2$, the Curie temperature T_C derived from the linear relationship between M^4 and H/M (see Fig. 9) equals 421 K, which is fully consistent with the value obtained from Arrott-Belov graphs (431 K). In $Sc_{1-x}Nb_xFe_2$ series of compound, M^4 vs H/M plots are linear near the critical point for Sc-rich compositions $x \leqslant 0.4$. However, for the Nb-rich side of the solid solution ($x > 0.4$) M^4 vs H/M curves become nonlinear, pointing out the contribution of the terms above the sixth order in the magnetic free energy in the vicinity of the critical temperature. As a result, determining the T_A parameter from Eq. (10) is no longer applicable in this concentration range $x > 0.4$ [32,62].

TABLE II. Spin-fluctuation parameters of $Sc_{1-x}Nb_xFe_2$. Comparison of the values of F_1, T_0, and T_A estimated at the ground state and T_A^* estimated at the critical region, and T_A^{**} determined using Eq. (11). The Curie temperatures used in the fitting are also given.

x	T_C (K)	F_1 (K)	T_0 (K)	T_A (K)	T_A^* (K)	T_A^{**} (K)
0	530 (5)	2047	2783	4584	4178	4632
0.10	524 (5)	3294	1790	4703	3932	3825
0.15	443 (5)	4095	1166	4232	3380	2839
0.17	438 (5)	4466	1109	4309	3506	3082
0.175	432 (5)	3489	1121	3830	3370	2513
0.18	434 (5)	4785	917	4057	3419	2568
0.20	420 (5)	4265	933	3862	3339	2262
0.22	417 (5)	4047	893	3680	3218	2184
0.25	383 (5)	3466	983	3574	3105	2106
0.30	345 (5)	822	2240	2628	2869	1918
0.35	314 (5)	427	6219	3157	2818	3335
0.40	240 (5)	756	7243	4532	2642	5481

In the limit of low temperature, the spontaneous moment squared is given as follows [31,32]:

$$\left(\frac{p_s(T)}{p_s(0)}\right)^2 = 1 - \frac{a_0}{p_s^4}\left(\frac{T}{T_A}\right)^2, \tag{11}$$

where $a_0 \approx 112.1$. The parameter T_A can be evaluated from the initial slope of $(\frac{p_s(T)}{p_s(0)})^2$ as a function of T^2 in the low-temperature region using Eq. (11). The resulting T_A values are listed in Table II and marked with T_A^{**}.

The spin-fluctuation parameters F_1, T_0, and T_A were determined using the above-mentioned methods; the corresponding values are listed in Table II. The T_A values estimated at low temperatures from Arrott-Belov graphs M^2 vs H/M, and those determined in the critical region from M^4 vs H/M plots, are of the same order of magnitude. Both parameters, T_A and T_0, are much larger than T_C, a feature usually observed in weakly ferromagnetic systems [61]. As shown in Table II, the concentration dependence of T_0 parameter of $Sc_{1-x}Nb_xFe_2$ alloys is nonmonotonic, namely, T_0 decreases in the low-concentration range and then increases for $x > 0.25$. This behavior is consistent with the drop in spontaneous magnetization above $x = 0.25$ observed previously in these intermetallics [45]. Interestingly, a similar behavior of T_0 was reported for $Y(Co_{1-x}Al_x)_2$ compounds by Yoshimura et *al.* [42]. Their study revealed that T_A and T_0 have a minimum value around the concentration where the ordered magnetic moment p_s has the maximum value. Note that in the (Sc, Nb)Fe_2 pseudobinary system, the isothermal magnetization curves for the compounds with $x > 0.3$ are not saturated even under the maximum attainable field of 10 T. This no saturation character of the magnetization isotherms leads to an inaccurate determination of the spin-fluctuation parameters. As shown in Table II, the value of T_0 for $x = 0.35$ and 0.4 compounds is about three times larger than that for alloys with $x \leqslant 0.3$. This rise in T_0 indicates an increase in the energy width of the 3*d* band. Consequently, the 3*d* Fe magnetism of the (Sc, Nb)Fe_2 system gradually weakens upon increasing Nb content, until the magnetic ordering disappears completely for $x = 1$.

Takahashi showed that there is a universal relationship between the $p_{\rm eff}/p_s$ ratio and T_C/T_0, Eq. (12) [32,41]. Additionally, he proposed generalized Rhodes-Wohlfarth plot to distinguish between weakly ferromagnetic materials and those exhibiting localized magnetism:

$$\frac{p_{\rm eff}}{p_s} \approx 1.4 \times \left(\frac{T_0}{T_C}\right)^{3/2}. \tag{12}$$

The theory of spin fluctuations was developed by Takahashi for quasi-two-dimensional itinerant ferromagnetic systems [63]. A parameter ε^2 was introduced as the ratio of the effective masses (m and m') for electron motion in the *by* plane and along the *z* axis, respectively. This ε^2 parameter equals 1 and 0 for the two limiting cases of three-dimensional (3D) and two-dimensional (2D) systems, respectively [63].

Figure 10 presents the generalized Rhodes-Wohlfarth plot and Fig. 11 displays the Deguchi-Takahashi log-log plot [32] for (Sc, Nb)Fe_2 compounds and other ferromagnetic systems. The blue line in Figs. 10 and 11 corresponds to the universal relationship, Eq. (12). The dotted lines represent Takahashi's relationship for values of $\varepsilon^2 = 0.2$ and 0.05. These curves are taken from Ref. [44] in order to compare our results with Takahashi's theoretical model. The Deguchi-Takahashi plot allows to identify the degree of itinerancy of magnetism and the dimensionality of spin fluctuations within a series of ferromagnetic materials. In the present case, Nb for Sc substitution results in an increase of the degree of itinerancy of 3*d* Fe magnetism along the $Sc_{1-x}Nb_xFe_2$ series of compounds (see Fig .10). With respect to the dimensionality of spin fluctuations in this family, Fig. 11 demonstrates that 3D fluctuations dominate for Sc-rich compounds. In contrast, the systems on the Nb-rich side behave as materials in which the quasi-2D fluctuation amplitude is dominant, the corresponding points being close to the curve for $\varepsilon^2 = 0.05$. On

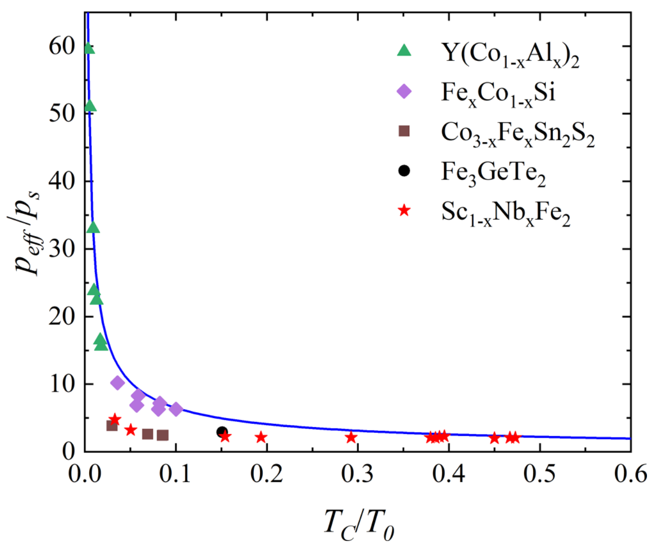

FIG. 10. Generalized Rhodes-Wohlfarth plot for $Sc_{1-x}Nb_xFe_2$ and various itinerant ferromagnets, such as $Y(Co_{1-x}Al_x)_2$ [60], $Fe_xCo_{1-x}Si$ [60], $Co_{3-x}Fe_xSn_2S_2$ [44], and Fe_3GeTe_2 [43]. Blue solid line represents the theoretical Eq. (12) proposed by Takahashi.

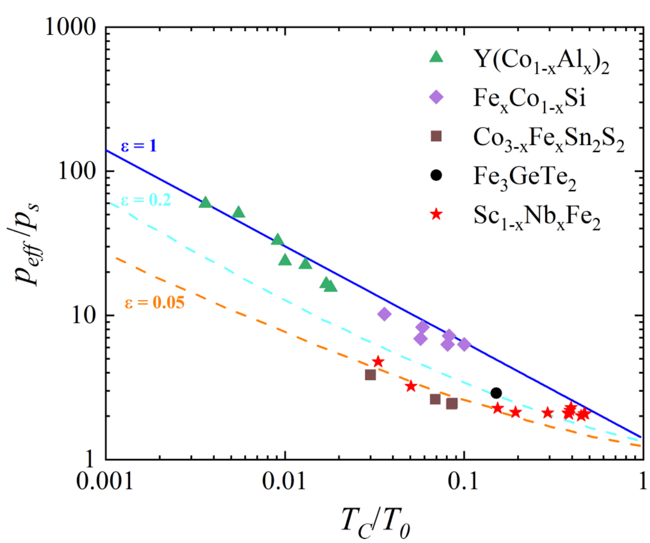

FIG. 11. Deguchi-Takahashi plot for $Sc_{1-x}Nb_xFe_2$ and various itinerant ferromagnets [43,44,60]. Blue solid line represents the theoretical Eq. (12) with $\varepsilon = 1$ and the dashed lines for $\varepsilon = 0.2$ and $\varepsilon = 0.05$ [44].

the basis on the crystal and magnetic structures depicted in Fig. 1, the system has three-dimensional character and one would expect the spin fluctuations to remain predominantly 3D. Yet, it is well established that the presence of a weak magnetocrystalline anisotropy can induce a deviation from the theoretical curve ($\varepsilon^2 = 1$) of the 3D ferromagnets [32,64]. The difficulty of observing pure 2D critical behaviors is specific to weak itinerant-electron ferromagnets [65,63] and has been proved by Ikeda and co-workers [65], who studied a weak ferromagnet with a quasi-two-dimensional layered crystal structure, where no definite 2D fluctuation behavior has been observed. The spin-fluctuation theory of quasi-two-dimensional itinerant-electron ferromagnets shows that quasi-2D itinerant weak magnets will behave qualitatively like 3D magnets [63]. (Sc, Nb)Fe_2 intermetallics clearly depart from the behavior described by Eq. (12); further single-crystal magnetic measurements and theoretical investigations may be of interest to understand the origin of the behavior observed in Fig. 11 for this series of compounds.

IV. CONCLUSION

The detailed investigation of the magnetic properties of $Sc_{1-x}Nb_xFe_2$ series of compounds reveals that in spite of the apparent simplicity of such model system, a strong evolution of the magnetism occurs upon Nb for Sc substitution. Whereas both Nb and Sc are nonmagnetic, large changes are observed on the Fe itinerant-electron magnetic behavior. First, a remarkable drop of the ordering temperature is observed upon increasing Nb content together with a vanishing of the magnetization. The thermal dependence of the magnetization has been fitted using Kuz'min's relation; it clearly demonstrates an evolution from a short-range ferromagnetic system for $ScFe_2$ towards systems with competing exchange interactions when Nb is substituted for Sc. Composition dependence of the shape parameter s indicates an evolution of the $3d$ magnetism with reduction of ferromagnetic exchange interaction and possible reinforcement of antiferromagnetic-type interactions. The study in the paramagnetic state indicates a pronounced reduction of the Curie-Weiss temperature as well as a progressive increase of the effective magnetic moment. Comparison of the different compounds using a Rhodes-Wohlfarth-type plot clearly revealed an evolution from mostly localized magnetic character of Fe moments to a strongly delocalized one upon increasing the Nb content along the $Sc_{1-x}Nb_xFe_2$ series of compounds. It is deduced that the transverse spin fluctuations are dominant for $ScFe_2$ whereas the longitudinal one progressively increases for the richest Nb compositions, which evolve progressively towards the weak ferromagnetic limit. The magnetization curves have also been analyzed using Takahashi's theoretical model, the analysis of which confirms this tendency. Spin-fluctuation parameters T_A and T_0 are above the Curie temperature value for all $Sc_{1-x}Nb_xFe_2$ compounds, and the evolution of T_C/T_0 and p_{eff}/p_s ratios as a function of Nb content indicates a tendency towards itinerant magnetism when Nb is substituted for Sc. This behavior was observed by plotting these compounds on the universal Deguchi-Takahashi plot.

[1] J. J. M. Franse and R. J. Radwański, in *Handbook of Magnetic Materials*, edited by K. H. J. Buschow (Elsevier, 1993), Chap. 5, Vol. 7, pp. 307–501.

[2] F. Stein and A. Leineweber, Laves phases: A review of their functional and structural applications and an improved fundamental understanding of stability and properties, J. Mater. Sci. **56**, 5321 (2021).

[3] B. Li, X. H. Luo, H. Wang, W. J. Ren, S. Yano, C.-W. Wang, J. S. Gardner, K.-D. Liss, P. Miao, S.-H. Lee, T. Kamiyama, R. Q. Wu, Y. Kawakita, and Z. D. Zhang, Colossal negative thermal expansion induced by magnetic phase competition on frustrated lattices in Laves phase compound (Hf, Ta)Fe_2, Phys. Rev. B **93**, 224405 (2016).

[4] V. Paul-Boncour and T. Mazet, Investigation of compounds for magnetocaloric applications: $YFe_2H_{4.2}$, $YFe_2D_{4.2}$, and $Y_{0.5}Tb_{0.5}Fe_2D_{4.2}$, J. Appl. Phys. **105**, 013914 (2009).

[5] V. Paul-Boncour, M. Guillot, G. Wiesinger, and G. André, Giant isotope effect on the itinerant-electron metamagnetism in $YFe_2(H_yD_{1-y})_{4.2}$, Phys. Rev. B **72**, 174430 (2005).

[6] O. Isnard, V. Paul-Boncour, and Z. Arnold, On the origin of the giant isotopic effect of hydrogen on the magnetic properties of $YFe_2A_{4.2}$ (A = H, D): A high pressure study, Appl. Phys. Lett. **102**, 122408 (2013).

[7] H. R. Rechenberg, L. Morellon, P. A. Algarabel, and M. R. Ibarra, Magnetic moment at highly frustrated sites of antiferromagnetic Laves phase structures, Phys. Rev. B **71**, 104412 (2005).

[8] T. Nakamichi, Ferro- and antiferromagnetism of the Laves phase compound in Fe-Ti alloy system, J. Phys. Soc. Jpn. **25**, 1189 (1968).

[9] L. V. B. Diop, J. Kastil, O. Isnard, Z. Arnold, and J. Kamarad, Collapse of ferromagnetism in itinerant-electron system: A magnetic, transport properties, and high pressure study of (Hf, Ta)Fe_2 compounds, J. Appl. Phys. **116**, 163907 (2014).

[10] T. Nakamichi, K. Kai, Y. Aoki, K. Iekda, and M. Yamamoto, Ferromagnetism in the Laves phase compound $Fe_{2+x}Hf_{1-x}$ annealed at 1000 °C, J. Phys. Soc. Jpn. **29**, 794 (1970).

[11] K. Ikeda, T. Nakamichi, T. Yamada, and M. Yamamoto, Ferromagnetism in Fe_2Sc with the hexagonal $MgZn_2$-type structure, J. Phys. Soc. Jpn. **36**, 611 (1974).

[12] A. Alam and D. D. Johnson, Chemically mediated quantum criticality in $NbFe_2$, Phys. Rev. Lett. **107**, 206401 (2011).

[13] M. Brando, W. J. Duncan, D. Moroni-Klementowicz, C. Albrecht, D. Grüner, R. Ballou, and F. M. Grosche, Logarithmic Fermi-liquid breakdown in $NbFe_2$, Phys. Rev. Lett. **101**, 026401 (2008).

[14] T. D. Haynes *et al.*, Ferrimagnetism in Fe-rich $NbFe_2$, Phys. Rev. B **85**, 115137 (2012).

[15] S. Friedemann, M. Brando, W. J. Duncan, A. Neubauer, C. Pfleiderer, and F. M. Grosche, Ordinary and intrinsic anomalous Hall effects in $Nb_{1-y}Fe_{2+y}$, Phys. Rev. B **87**, 024410 (2013).

[16] D. Moroni-Klementowicz, M. Brando, C. Albrecht, W. J. Duncan, F. M. Grosche, D. Grüner, and G. Kreiner, Magnetism

in $Nb_{1-y}Fe_{2+y}$: Composition and magnetic field dependence, Phys. Rev. B **79**, 224410 (2009).
[17] A. Subedi and D. J. Singh, Band structure and itinerant magnetism in quantum critical $NbFe_2$, Phys. Rev. B **81**, 024422 (2010).
[18] S. Friedemann, W. J. Duncan, M. Hirschberger, T. W. Bauer, R. Küchler, A. Neubauer, M. Brando, C. Pfleiderer, and F. M. Grosche, Quantum tricritical points in $NbFe_2$, Nat. Phys **14**, 62 (2018).
[19] L. Sun, H. Yibole, O. Tegus, and F. Guillou, Magnetocaloric effect, magnetoresistance of $Sc_{0.28}Ti_{0.72}Fe_2$, and phase diagrams of $Sc_{0.28}Ti_{0.72}Fe_{2-x}T_x$ alloys with T = Mn or Co, Crystals **10**, 410 (2020).
[20] M. Saoudi, J. Déportes, and B. Ouladdiaf, Magnetic ground state of $Ti_{1-x}Sc_xFe_2$ system, J. Magn. Magn. Mater. **231**, 265 (2001).
[21] Y. Nishihara and Y. Yamaguchi, Magnetic properties of the $(Sc_{1-x}Ti_x)Fe_2$ system having two magnetic states with different degrees of localization, J. Phys. Soc. Jpn. **55**, 920 (1986).
[22] H. Yibole, A. K. Pathak, Y. Mudryk, F. Guillou, N. Zarkevich, S. Gupta, V. Balema, and V. K. Pecharsky, Manipulating the stability of crystallographic and magnetic sub-lattices: A first-order magnetoelastic transformation in transition metal based Laves phase, Acta Mater. **154**, 365 (2018).
[23] L. V. B. Diop, O. Prokhnenko, O. Isnard, G. Ballon, and J. P. Itié, Investigation of the itinerant metamagnetic system $Hf_{0.75}Ta_{0.25}Fe_2$ under extreme conditions of pressure or magnetic field, Intermetallics **129**, 107054 (2021).
[24] F. Sayetat, J. Déportes, B. Ouladdiaf, M. Kessler, M. Saoudi, and M. Reehuis, Fe magnetism in $Ti_{1-x}Sc_xFe_2$ ($x \leqslant 0.2$)1, J. Magn. Magn. Mater. **192**, 100 (1999).
[25] L. V. B. Diop, D. Benea, S. Mankovsky, and O. Isnard, Cross over between ferro and antiferromagnetic order in Fe itinerant electron magnetism: An experimental and theoretical study of the model (Hf, Ta)Fe_2 Laves phases, J. Alloys Compd. **643**, 239 (2015).
[26] P. Bag, R. Rawat, P. Chaddah, P. D. Babu, and V. Siruguri, Unconventional thermal effects across first-order magnetic transition in the Ta-doped $HfFe_2$ intermetallic, Phys. Rev. B **93**, 014416 (2016).
[27] H. Nishihara, G. Kido, Y. Nishihara, M. Itoh, and H. Yasuoka, Magnetization process of $Hf_{0.8}Ta_{0.2}Fe_2$ in strong pulsed magnetic fields, Solid State Commun. **49**, 1113 (1984).
[28] Y. Nishihara and Y. Yamaguchi, Magnetic phase transitions in itinerant electron magnets $Hf_{1-x}Ta_xFe_2$, J. Phys. Soc. Jpn. **52**, 3630 (1983).
[29] T. Moriya and K. Usami, Coexistence of ferro- and antiferromagnetism and phase transitions in itinerant electron systems, Solid State Commun. **23**, 935 (1977).
[30] K. Yoshimura, Theme of the workshop on itinerant-electron magnetism, and spin fluctuations, J. Phys.: Conf. Ser. **868**, 012001 (2017).
[31] Y. Takahashi, Theoretical development in itinerant electron ferromagnetism, J. Phys.: Conf. Ser. **868**, 012002 (2017).
[32] Y. Takahashi, *Spin Fluctuation Theory of Itinerant Electron Magnetism* (Springer, Berlin, 2013), Vol. 253.
[33] F. Bloch, Bemerkung zur Elektronentheorie des Ferromagnetismus und der elektrischen Leitfähigkeit, Z. Phys. **57**, 545 (1929).
[34] J. C. Slater, The ferromagnetism of nickel, Phys. Rev. **49**, 537 (1936).
[35] J. C. Slater, The ferromagnetism of nickel. II. Temperature effects, Phys. Rev. **49**, 931 (1936).
[36] E. C. Stoner, Collective electron ferronmagnetism, Proc. R. Soc. Lond, Astron. **165**, 372 (1938).
[37] E. C. Stoner, Collective electron ferromagnetism II. Energy and specific heat, Proc. R. Soc. Lond, Astron. **169**, 339 (1939).
[38] P. Rhodes and E. P. Wohlfarth, The effective Curie-Weiss constant of ferromagnetic metals and alloys, Proc. R. Soc. Lond, Astron. **273**, 247 (1963).
[39] T. Moriya and A. Kawabata, Effect of spin fluctuations on itinerant electron ferromagnetism, J. Phys. Soc. Jpn. **34**, 639 (1973).
[40] T. Moriya and A. Kawabata, Effect of spin fluctuations on itinerant electron ferromagnetism. II, J. Phys. Soc. Jpn. **35**, 669 (1973).
[41] Y. Takahashi, On the origin of the Curie-Weiss law of the magnetic susceptibility in itinerant electron ferromagnetism, J. Phys. Soc. Jpn. **55**, 3553 (1986).
[42] K. Yoshimura, M. Takigawa, Y. Takahashi, H. Yasuoka, and Y. Nakamura, NMR study of weakly itinerant ferromagnetic $Y(Co_{1-x}Al_x)_2$, J. Phys. Soc. Jpn. **56**, 1138 (1987).
[43] B. Chen, J. Yang, H. Wang, M. Imai, H. Ohta, C. Michioka, K. Yoshimura, and M. Fang, Magnetic properties of layered itinerant electron ferromagnet Fe_3GeTe_2, J. Phys. Soc. Jpn. **82**, 124711 (2013).
[44] M. A. Kassem, Y. Tabata, T. Waki, and H. Nakamura, Quasi-two-dimensional magnetism in Co-based shandies, J. Phys. Soc. Jpn. **85**, 064706 (2016).
[45] S. El Bidaoui, L. V. B. Diop, F. Maccari, and O. Isnard, A structural study and some magnetic properties of the (Sc, Nb)Fe_2 series of compounds, J. Alloys Compd. **985**, 174013 (2024).
[46] E. P. Wohlfarth, Magnetic properties of crystalline and amorphous alloys: A systematic discussion based on the Rhodes-Wohlfarth plot, J. Magn. Magn. Mater. **7**, 113 (1978).
[47] A. Barlet, J. C. Genna, and P. Lethuillier, Insert for regulating temperatures between 2 and 1000 K in a liquid helium dewar: Description and cryogenic analysis, Cryogenics **31**, 801 (1991).
[48] E. Burzo and F. Givord, Comportement paramagnetique des atomes de fer dans quelques composes intermetalliques avec l'yttrium, le lutecium et le gadolinium, C. R. Acad. Sci. Paris **271B**, 1159 (1970).
[49] O. Isnard, V. Pop, and K. H. J. Buschow, Magnetic properties of $Th_2Fe_{17}C_x$ compounds (x = 0, 0.6, 0.9, 1.1), J. Appl. Phys. **101**, 103908 (2007).
[50] Y. Nishihara and Y. Yamaguchi, Magnetic structures in the $Sc_{1-x}Ti_xFe_2$ system–magnetic phase transitions in itinerant electron systems, J. Phys. Soc. Jpn. **54**, 1122 (1985).
[51] E. Burzo, On the magnetism of Fe and Co in rare-earth (yttrium) compounds, Balkan Phys. Lett. **5**, 208 (1997).
[52] T. Moriya and Y. Takahashi, Spin fluctuation theory of itinerant electron ferromagnetism –A unified picture, J. Phys. Soc. Jpn. **45**, 397 (1978).
[53] L. V. B. Diop, Structure et Propriétés Physiques de Composés Magnétiques de Type $RT_{12}B_6$ et (Hf, Ta)Fe_2 et Leur Dépen-

dance En Fonction de La Pression (Physique Ou Chimique) (R = élément de Terre Rare et T = élément de Transition 3d), Ph.D. thesis, Grenoble, 2014.

[54] K. P. Belov and A. N. Georgia, Thermodynamical description of magnetization of ferromagnets near the Curie temperature, Fiz. Met. Metalloved **2**, 3 (1956).

[55] A. Arrott, Criterion for ferromagnetism from observations of magnetic isotherms, Phys. Rev. **108**, 1394 (1957).

[56] M. D. Kuz'min, Shape of temperature dependence of spontaneous magnetization of ferromagnets: Quantitative analysis, Phys. Rev. Lett. **94**, 107204 (2005).

[57] M. D. Kuz'min, M. Richter, and A. N. Yaresko, Factors determining the shape of the temperature dependence of the spontaneous magnetization of a ferromagnet, Phys. Rev. B **73**, 100401(R) (2006).

[58] M. D. Kuz'min, K. P. Skokov, L. V. B. Diop, I. A. Radulov, and O. Gutfleisch, Exchange stiffness of ferromagnets, Eur. Phys. J. Plus **135**, 301 (2020).

[59] B. Vallet-Simond, L. V. B. Diop, and O. Isnard, Magnetism of 3d electrons in $YCo_{12-x}Fe_xB_6$ compounds, J. Magn. Magn. Mater. **587**, 171307 (2023).

[60] Y. Takahashi, Quantum spin fluctuation theory of the magnetic equation of state of weak itinerant-electron ferromagnets, J. Phys.: Condens. Matter **13**, 6323 (2001).

[61] K. Yoshimura, M. Mekata, M. Takigawa, Y. Takahashi, and H. Yasuoka, Spin fluctuations in $Y(Co_{1-x}Al_x)_2$: A transition system from nearly to weakly itinerant ferromagnetism, Phys. Rev. B **37**, 3593 (1988).

[62] K. Moriyama, J. Murakawa, H. Kanagawa, C. Michioka, H. Ueda, H. Michor, and K. Yoshimura, Ferromagnetic Spin Fluctuation in the Itinerant-Electron Magnetic Compounds RCo_9Si_4 (R = Y, La), Powder Metall. **69**, 467 (2022).

[63] Y. Takahashi, Spin-fluctuation theory of quasi-two-dimensional itinerant-electron ferromagnets, J. Phys.: Condens. Matter **9**, 10359 (1997).

[64] M. Imai, C. Michioka, H. Ueda, and K. Yoshimura, Static and dynamical magnetic properties of the itinerant ferromagnet $LaCo_2P_2$, Phys. Rev. B **91**, 184414 (2015).

[65] S. Ikeda, Y. Maeno, and T. Fujita, Weak ferromagnetism in two-dimensional bilayered $Sr_{3-x}Ca_xRu_2O_7$, Phys. Rev. B **57**, 978 (1998).